JOURNAL OF CATALYSIS **169,** 93–102 (1997)
ARTICLE NO. CA971681

Copper Ion-Exchanged SAPO-34 as a Thermostable Catalyst for Selective Reduction of NO with C_3H_6

Tatsumi Ishihara,[1] Masaru Kagawa, Fumiaki Hadama, and Yusaku Takita

Department of Applied Chemistry, Faculty of Engineering, Oita University, Dannoharu 700, Oita, 870-11, Japan

Received September 11, 1995; revised December 19, 1996; accepted February 28, 1997

Selective reduction of NO with C_3H_6 in the presence of oxygen was studied over Cu ion-exchanged SAPO-*n* ($n = 5$, 11, 34), and Cu ion-exchanged Zeolites β, USY, and ZSM-5. All the Cu ion-exchanged catalysts exhibited high activity for NO reduction with C_3H_6 in a large excess of O_2; however, the temperature for maximum NO conversion depended on the kind of molecular sieve. Although the maximum conversion of NO was attained at a slightly higher temperature in comparison with Cu–ZSM-5, Cu–SAPO-34 exhibited the highest activity for NO reduction among the catalysts studied under the conditions examined. Furthermore, high NO conversion was attained over a wide temperature range, from 623 to 873 K. SAPO-34 has high thermal stability. High activity for NO selective reduction on Cu–SAPO-34 was sustained for more than 60 h at 673 K in an atmosphere containing 15 vol% H_2O. After thermal treatment at 1073 K in humidified atmosphere, the decrease in activity for NO reduction was also small. Redox behavior of Cu ions in SAPO-34 between monovalent and divalent states occurs during the selective reduction of NO, and the reaction seems to proceed via formation of adsorbed nitrate species followed by the formation of organic nitro compounds.

1. INTRODUCTION

Aluminophosphates ($AlPO_4$-*n*) are a new family of molecular sieves that possess the characteristics of a molecularsized pore structure and solid acidity. In particular, $AlPO_4$-*n* exhibits extremely high thermal stability as compared with synthetic zeolites. It was reported that the crystal structure of $AlPO_4$-5 is retained up to 1473 K (1). Similarly, the crystal structure of SAPO-34 is sustained up to 1273 K, even in the presence of humidity (2). Silicoaluminophosphates (SAPO-*n*) exhibit cation-exchange properties as a result of the isomorphous substitution of P in $AlPO_4$ by Si. Therefore, $AlPO_4$-*n* and SAPO-*n* have great possibilities as thermostable catalysts; however, the advantages in thermal stability of SAPO-*n* or $AlPO_4$-*n* have not yet been thoroughly exploited in conventional studies.

Selective reduction of NO_x under an oxidizing atmosphere with hydrocarbons has attracted attention as a new process for the catalytic removal of NO_x in the exhaust gas of diesel or lean-burn engines (3–6). It is reported that Cu ion-exchanged ZSM-5 is highly active for the selective reduction of NO (7); however, the high activity of Cu–ZSM-5 to NO reduction decreases gradually with time-on-stream at temperatures higher than 973 K. One reason for the decrease in activity seems to be the poor thermal stability of ZSM-5 (8–10). In addition, dealumination easily proceeds on ZSM-5 under a humidified atmosphere, resulting in accelerating decreases in the activity for NO_x reduction. We have investigated Cu ion-exchanged SAPO-*n* for the selective reduction of NO and have found that Cu–SAPO-34 exhibits high activity for NO reduction with C_3H_6 (11). The state of ion-exchanged Cu in SAPO-34 and its catalytic properties are also being studied by other groups (12, 13). In this paper, the activities of Cu–SAPO-*n* ($n = 5$, 11, and 34) for NO_x reduction with C_3H_6 in the presence of O_2 are further studied as a thermostable NO_x removal catalyst. Moreover, the oxidation states of the copper ions in SAPO-34 on treatment with C_3H_6, NO, and O_2 in the working state have been studied to explore the mechanism of the selective reduction of NO with C_3H_6.

2. EXPERIMENTAL

Catalyst Preparation

SAPO-5, 11, and 34, (Si, Al, and P contents: 1.77, 12.09, and 10.03 mmol g^{-1}, respectively) and zeolite β ($SiO_2/Al_2O_3 = 26$) were synthesized according to U.S. patents (14, 15). To prepare SAPO-*n*, colloidal SiO_2, Al compound [pseudo-boehmite phase (Cataloid AP, Catalysis & Chemical Ind.) for SAPO-5 and SAPO-11, $Al[OCH(CH_3)_2]_3$ for SAPO-34], phosphoric acid (85%), and template amine (triethylamine for SAPO-5, di-*n*-propylamine for SAPO-11, and 10% tetraethylammonium hydroxide for SAPO-34) were mixed at room temperature for a few hours. The precursor of SAPO-*n* obtained in this way was heated (453 K, 12 h for SAPO-5 and SAPO-11, 483 K, 24 h for SAPO-34) in autoclaves (Taiatsu Glass TAF-150) in which all parts were coated with Teflon. The synthesized SAPO-*n* and zeolite β, as well

[1] To whom correspondence should be sent. Fax: +81-975-54-7979.

0021-9517/97 $25.00

as the commercial ZSM-5 (Mobil, $SiO_2/Al_2O_3 = 30$) and USY (Catalysis & Chemical Ind., $SiO_2/Al_2O_3 = 17$), were ion-exchanged with Cu^{2+} in a 0.01 *M* Cu^{2+} acetate aqueous solution. At the final stage of Cu ion exchange, ammonia water was added to adjust the pH to 7.5 to control the amount of Cu ion-exchanged. Exchanged amounts of Cu^{2+} for each type of SAPO-*n*, *β*, USY, and ZSM-5 were estimated to be about 3 wt% from ICP analysis. In the case of SAPO-*n*, this amount of Cu corresponds to ca. 75% of the formula ion-exchange capacity, which is estimated by assuming that all the Si forms ion-exchange sites. Before measurement of the activity for NO reduction with C_3H_6, the catalysts were calcined at 773 K for 4 h in a He stream.

NO Reduction with C_3H_6

The catalytic activities for NO reduction were measured with a fixed-bed microflow reactor. A gas mixture consisting of NO (5000 or 1000 ppm), C_3H_6 (1000 ppm), O_2 (5%), and He (remainder) was fed to the catalyst bed at $W/F =$ 0.3 g-cat · s cm^{-3} (Space velocity = ca. 8500 h^{-1}), where *W* and *F* stand for catalyst weight and flow rate, respectively. Conversion to N_2 was estimated from analysis of the N_2 concentration in the flue gases by gas chromatography. The heat resistances of SAPO-*n* and ZSM-5 were determined by calcining at a prescribed temperature for 2 h in air containing 3 vol% H_2O.

Characterization of Cu Ion-Exchanged SAPO-34

The valence of the Cu ions in SAPO-34 was determined by ESR (JEOL JEX-FE1X) and XPS (Shimadzu ESCA-850). Before the ESR measurement, the catalyst was evacuated at 773 K for 5 h, calcined in O_2 (100 Torr) at 673 K for 4 h, and then evacuated at 573 K for 4 h. The ESR measurement was performed at room temperature and diphenylpicrylhydrazyl (DPPH) was used as an external standard for the calibration of the *g* value. XPS measurement of the ion-exchanged Cu in SAPO-34 was performed after a calcination in oxygen (1 atm) at 623 K for 3 h in the pretreatment chamber. Magnesium *Kα* (1254.6 eV) was used as the X-ray source for measurement of the XPS of Cu $2p_{3/2}$ and the Auger line of Cu LMM. The binding energy of Cu $2p_{3/2}$ and the position of the LMM Auger peak were corrected by taking the binding energy of deposited Au $4f_{7/2}$ level as 84 eV.

Adsorption states of NO or C_3H_6 on Cu–SAPO-34 were investigated by infrared absorption spectroscopy (Hitachi 270 spectrometer). A sample disk (ca. 0.03 g) was heated at 773 K for 5 h *in vacuo* to remove water and other adsorbed gases. After calcination in O_2 (100 Torr) at 673 K for 4 h, the sample disk was exposed to the adsorbed gas (100 Torr) in an IR cell with KBr single-crystal windows. The background spectrum was subtracted from the IR spectra measured after adsorption treatment. A mass spectrometer (Anelva, AQA-100R) was connected to the IR cell for qualitative analysis of the gas phase during the adsorption treatment.

The crystal structure of Cu ion-exchanged SAPO-34 was analyzed by X-ray diffraction and NMR measurements. X-ray diffraction analysis (Rigaku, 2013CN) was performed with the Cu *Kα* line and NMR spectra for ^{27}Al, ^{31}P, and ^{29}Si were recorded with a Bruker APR-300 spectrometer operating at a field of 7 T using the magic-angle-spinning (MAS) technique. Spinning speeds of 5.5 kHz were used and the chemical shifts of Al, P, and Si were referred to the external standard of 1.5 *M* $Al(H_2O)_6^{3+}$ in $Al(NO_3)_3$ aqueous solution, H_3PO_4 (85%), and 4.5 *M* tetramethylsilane in benzene solution, respectively.

3. RESULTS AND DISCUSSION

Selective Reduction of NO with C_3H_6 on Metal Ion-Exchanged SAPO-n

Figure 1 shows the catalytic activity of Cu ion-exchanged SAPO-*n*, *β*, USY, and ZSM-5 as a function of reaction temperature. Since it is reported that Cu–ZSM-5 is active for direct decomposition of NO ($2NO = N_2 + O_2$), an excess amount of NO in comparison with that of C_3H_6 was fed in this experiment. Note, therefore, that the reaction conditions in Fig. 1 deviate strongly from the actual flue gases from vehicles. As reported, Cu–ZSM-5 exhibits high activity for NO reduction at 573 K and the activity decreases with increasing temperature (7). Since the SiO_2/Al_2O_3 ratio of the examined ZSM-5 is 30, which is higher than that of ZSM-5 examined by Hosose *et al.* (7), the NO reduction activity of Cu–ZSM-5 examined in this study was slightly lower than that of Cu–ZSM-5 previously reported (7), albeit

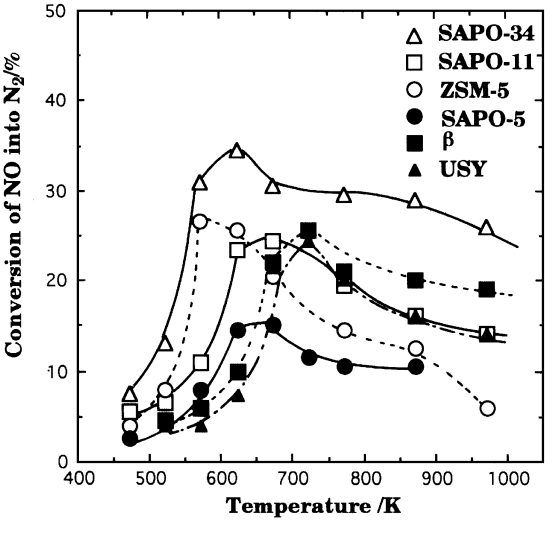

FIG. 1. Temperature dependence of catalytic activity of molecular sieves ion-exchanged with Cu for NO reduction with C_3H_6 ($P_{NO} =$ 5000 ppm, $P_{C_3H_6} = 1000$ ppm, $P_{O_2} = 5\%$, $W/F = 0.3$ g · s cm^{-3}).

with different reaction conditions. This may result from the different acidity of ZSM-5 resulting from the difference in the SiO_2/Al_2O_3 ratio. Zeolite β and USY ion-exchanged by Cu also exhibit a high activity to NO reduction; however, a temperature higher than 673 K was required to attain the high conversion to N_2. Although the temperature at which each Cu–SAPO-*n* attains maximum conversion to N_2 is higher than that of Cu–ZSM-5 by about 50 K, the activity of Cu–SAPO-*n* for NO reduction is comparable to that of Cu–ZSM-5, except for SAPO-5. In particular, Cu–SAPO-34 exhibits a higher activity to NO reduction than Cu–ZSM-5 over the entire temperature range, although the space velocity of the reactant is low. Furthermore, the high activity was sustained up to 873 K. Therefore, conversion to N_2 is twice higher on Cu–SAPO-34 than on Cu–ZSM-5 at 873 K. Since Cu–SAPO-34 exhibited the highest activity to NO reduction with C_3H_6 among the catalysts examined, catalytic activity for NO reduction and thermal stability were investigated on SAPO-34 in this study.

It has been reported that the activity of ZSM-5 is strongly affected by the ion-exchanged metal cation (16). Figure 2 shows the effects of the metal cation on the NO reduction activity of SAPO-34. Reduction of NO with C_3H_6 proceeded on all metal cation-exchanged SAPO-34 and almost the same maximum conversion of NO to N_2 was exhibited; however, the temperature at maximum NO conversion occurred depended strongly on the metal cations ion-exchanged. Fe–SAPO-34 exhibited high activity in a low temperature range from 473 to 873 K. On the other hand, high activity was attained at temperatures higher than 873 K on Ag–SAPO-34. Among the metal cations examined in this study, copper is the most suitable as an ion-exchanged

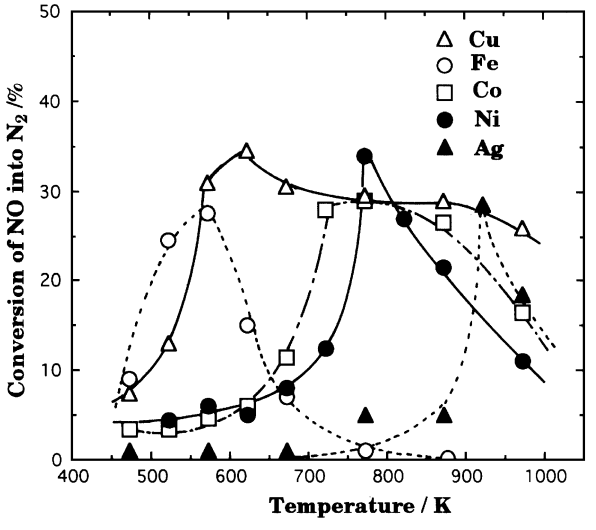

FIG. 2. Effects of different metal cations ion-exchanged in SAPO-34 on the catalytic activity for NO reduction with C_3H_6. The loading of metal is 3.0 wt% ($P_{NO} = 5000$ ppm, $P_{C_3H_6} = 1000$ ppm, $P_{O_2} = 5\%$, $W/F = 0.3$ g · s cm^{-3}).

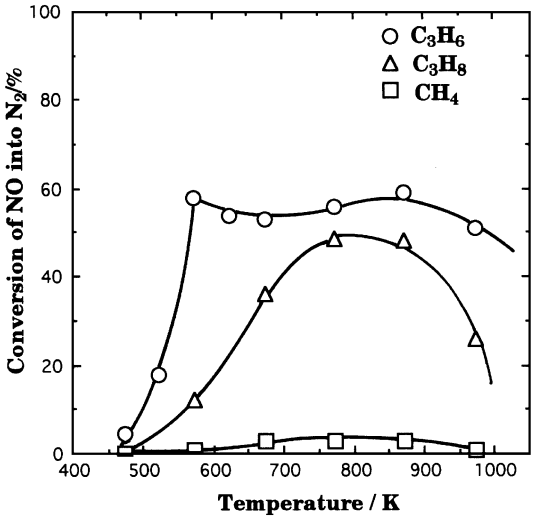

FIG. 3. Effects of different hydrocarbons as reductant on the activity of Cu–SAPO-34 for NO reduction ($P_{NO} = 1000$ ppm, $P_{hydrocarbon} = 1000$ ppm, $P_{O_2} = 5\%$, $W/F = 0.3$ g · s cm^{-3}).

cation for SAPO-34, considering the activity and temperature range of high NO conversion.

The activity of Cu–SAPO-34 for NO reduction is strongly dependent on the kind of hydrocarbon used as a reductant (Fig. 3). Although high activity for NO reduction was obtained over a wide temperature range by using C_3H_6 for reductant, the reaction temperature at high NO conversion was shifted to a higher temperature range and became narrow by using C_3H_8. On the other hand, selective reduction of NO to N_2 hardly proceeded when using CH_4 for reductant. The different influences of hydrocarbons as reductants on the activity of Cu–SAPO-34 for NO reduction seem to result from the differences in combustibility, since N_2 began to form on commencement of the oxidation of the hydrocarbons. It is expected that high conversion in NO reduction can be attained on Cu–SAPO-34 by using for reductant various kinds of hydrocarbons, except hydrocarbons with low combustibility such as CH_4.

Figure 4 shows NO conversion to N_2 as a function of the amount of Cu ion-exchanged. Since the number of ion-exchange sites is not completely correlated with the amount of Si in the case of SAPO-*n*, the amount of Cu is expressed on the basis of weight percent. It is also noted that 3.5 wt% Cu corresponds to almost 100% ion-exchange level. Clearly, conversion of NO to N_2 increases with increasing amount of Cu ion-exchanged and attains a maximum around 4 wt%. Although maximum NO conversion was obtained at 4.5 wt%, the activity gradually decreased and the color of the catalyst changed from clear blue to black after reaction. This suggests that some copper ions are reduced and aggregate during reaction. This may result from the fact that the amount of Cu ion is in excess of the ion-exchange sites, because Si in the framework of SAPO-34

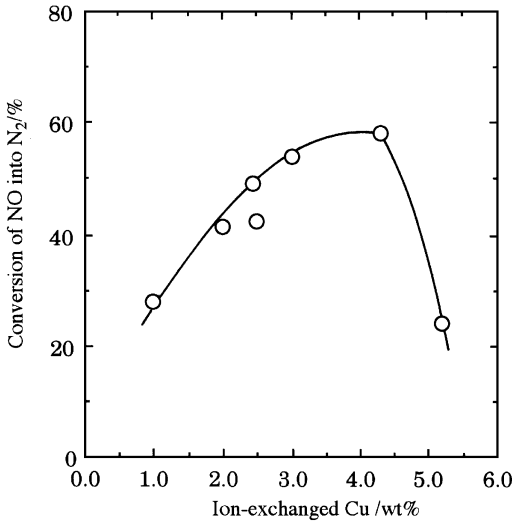

FIG. 4. NO conversion at 623 K as a function of the amount of Cu ion-exchanged ($P_{NO} = 1000$ ppm, $P_{C_3H_6} = 1000$ ppm, $P_{O_2} = 5\%$, $W/F = 0.3$ g·s cm^{-3}).

does not always form ion-exchange sites. This means that isomorphous substitution of Al with Si has also occurred in the case of SAPO-*n* (17). Consequently, the catalytic performance of Cu–SAPO-34 was studied in more detail with Cu–SAPO-34 at 3.0 wt%.

Thermal Stability of Cu–SAPO-34

Exhaust gases from engines contain humidity at high concentration. The influence of calcination in a humidified atmosphere on NO reduction activity is shown in Fig. 5. Although the activity of Cu–SAPO-34 to NO reduction was unaffected by the calcination up to 1073 K in a dry atmosphere, calcination at 1073 K in a humidified atmosphere decreased the activity for NO reduction. Therefore, the thermal stability of SAPO-34 is expected to decrease in the presence of H_2O; however, the extent of the decrease in the activity of Cu–SAPO-34 for NO reduction was relatively small, even after calcination at 1073 K in wet air, as shown in Fig. 5a. In contrast to Cu–SAPO-34, Cu–ZSM-5 became almost inactive by the same heat treatment, as shown in Fig. 5b. The thermal stability of SAPO-34 far exceeds that of the aluminosilicate, ZSM-5, since the crystal structure of synthesized SAPO-34 was sustained up to 1273 K, even in a wet atmosphere (2). Therefore, the thermal stability of Cu–SAPO-34 is satisfactorily high enough that it can be used as catalyst for automotive exhaust gases.

The changes in the crystal structure of SAPO-34 under NO reduction in a wet atmosphere were studied by XRD, as shown in Fig. 6. The XRD pattern in Fig. 6 indicates that the synthesized SAPO-34 is a single phase with good crystallinity (18). It is clearly shown that no changes can be recognized in XRD patterns of Cu–SAPO-34 prior to and after the NO reduction at 973 K for 5 h in an atmosphere containing 15 vol% H_2O. Moreover, degradation of crystals usually decreases the intensity of XRD peaks, and no such decrease was observed after NO reduction in a wet atmosphere. This suggests that the long-range order of SAPO-34 structure is stably sustained under NO reduction at temperatures as high as 973 K, even in an atmosphere containing H_2O.

Since no changes were observed in XRD patterns of SAPO-34 before and after reduction of NO at 973 K in a wet atmosphere, possible changes in the local structure of SAPO-34 ion-exchanged by Cu were investigated by NMR. Figure 7a shows the ^{27}Al-, ^{31}P-, and ^{29}Si-MAS NMR spectra of Cu–SAPO-34 prior to reduction of NO at 973 K for 5 h in an atmosphere containing 15 vol% H_2O. As-synthesized SAPO-34 exhibits MAS NMR spectra for Al, P, and Si similar to those previously reported (2). The resonance at 42 and −13 ppm in the ^{27}Al-NMR spectra seems to be that of a tetrahedral and an octahedral coordinated Al, respectively

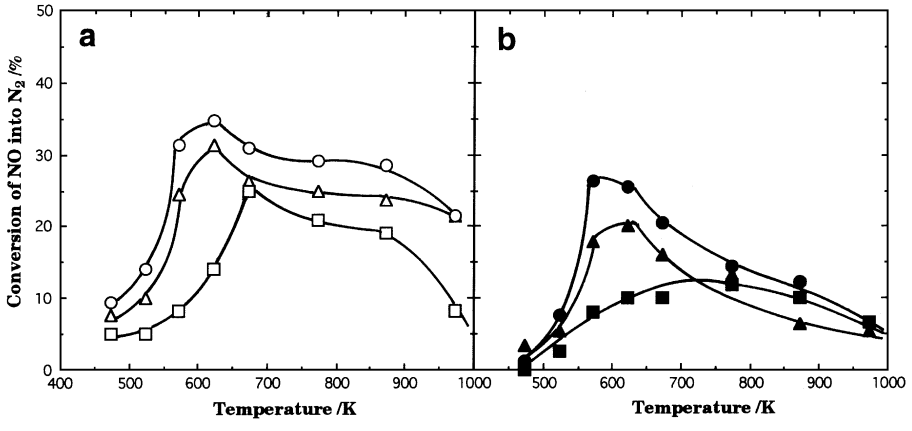

FIG. 5. Effects of heat treatment under an atmosphere containing 3 vol% H_2O on the activity for NO reduction with C_3H_6 ($P_{NO} = 5000$ ppm, $P_{C_3H_6} = 1000$ ppm, $P_{O_2} = 5\%$, $W/F = 0.3$ g·s cm^{-3}). (a) Cu–SAPO-34: (○) 773 K, (△) 973 K, (□) 1073 K. (b) Cu–ZSM-5: (●) 773 K, (▲) 973 K, (■) 1073 K.

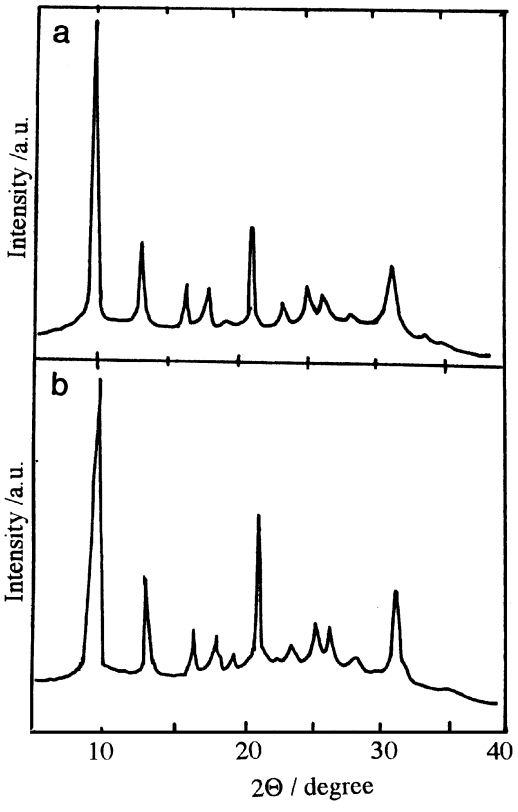

FIG. 6. X-ray diffraction patterns of Cu–SAPO-34 prior to or after NO reduction with C_3H_6 at 973 K for 5 h in an atmosphere containing 15 vol% H_2O. (a) Before reaction, (b) after reaction.

(2, 19). On the other hand, the ^{31}P-MAS NMR spectrum consists of a strong resonance line at −26 ppm and a broader line at −19 ppm, which could be assigned to a tetrahedral P without additional coordination or with water coordination, respectively (2, 20). Since the amount of Si is far smaller than that of Al or P, the intensity of the ^{29}Si-MAS NMR spectrum was weaker than those of P or Al; however, only one resonance due to tetrahedral Si was observed at −89 ppm in ^{29}Si-MAS NMR (2, 21, 22). This peak observed for Si-MAS NMR could be assigned to Si(4Al) according to the reports of Barthomeuf and co-workers (22). At the low concentration of Si in SAPO-*n*, added Si is isomorphously substituted for lattice P atoms; however, it is reported that the substitution of Si in the Al sites in addition to the P sites occurs at high Si content (23). In this study, the Si content in synthesized SAPO-34 was as low as 1.77 mmol g^{-1}. Consequently, all Si atoms added seem to substitute isomorphously at the lattice position of the P sites but not the Al sites. This is because only one kind of Si bonded with 4 Al atoms was recognized in ^{29}Si-MAS NMR spectra.

Figure 7b shows the MAS NMR spectra of ^{29}Si, ^{27}Al, and ^{31}P in Cu–SAPO-34 after NO reduction at 973 K, 5 h in a wet atmosphere. Although the relative intensity of peaks in ^{27}Al-NMR spectra was slightly changed, significant changes could not be observed in the MAS NMR spectra of Si, Al, and P. These MAS NMR studies clearly indicate that SAPO-34 ion-exchanged with Cu retained the crystal structure in short-range order as well as long-range order, even after NO reduction at a temperature as high as 973 K in coexistence with water vapor.

Figure 8 shows the temperature dependence of Cu–SAPO-34 for NO selective reduction with C_3H_6 prior to and after treatment at 973 K, 5 h in an atmosphere containing 15 vol% H_2O. It is clearly shown that the activity of Cu–SAPO-34 to NO reduction hardly varied after this heat treatment. These unchanged activities to NO reduction confirm the high thermal stability of the SAPO-34 crystal lattice which is shown by the NMR results.

Conversion of NO to N_2 was studied as a function of time-on-stream in the atmosphere containing 15 vol% H_2O (Fig. 9). Compared with the NO conversion in a dry atmosphere shown in Fig. 1, the presence of water decreased the NO conversion. This may result from the suppression of NO or C_3H_6 adsorption by the coadsorption of water; however,

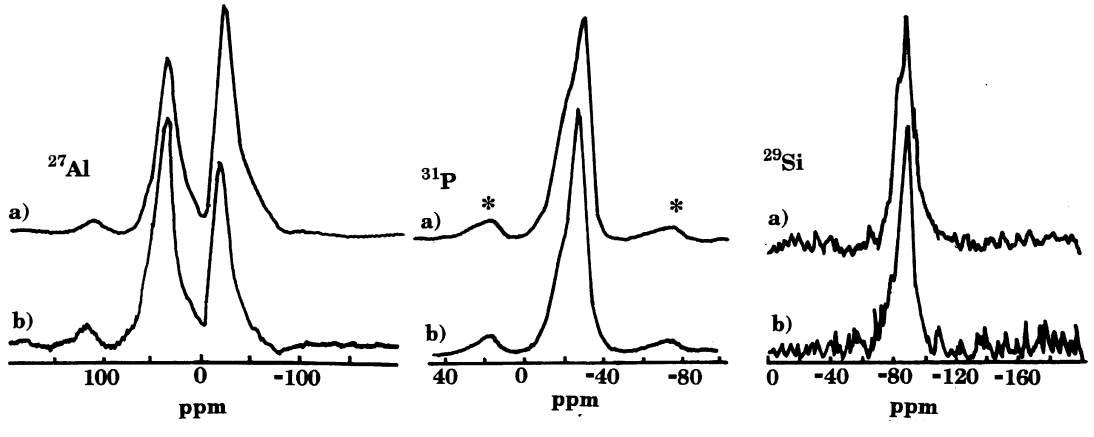

FIG. 7. MAS NMR spectra of Cu–SAPO-34 prior to or after NO reduction with C_3H_6 at 973 K for 5 h in an atmosphere containing 15 vol% H_2O. (a) Before reaction, (b) after reaction. *Spinning side band.

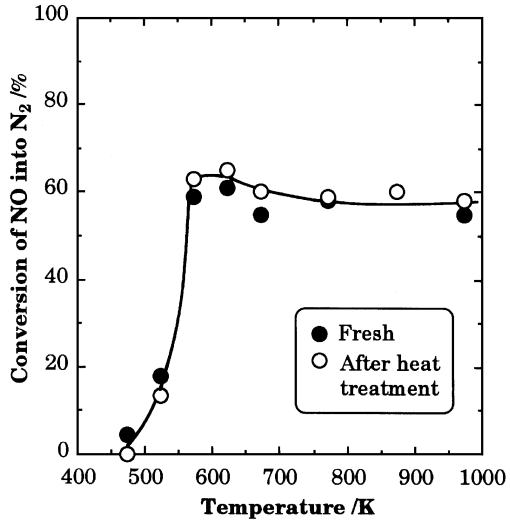

FIG. 8. Temperature dependence of Cu–SAPO-34 for NO selective reduction with C_3H_6 prior to and after calcination at 973 K for 5 h in an atmosphere containing 15 vol% H_2O ($P_{NO} = 1000$ ppm, $P_{C_3H_6} = 1000$ ppm, $P_{O_2} = 5\%$, $W/F = 0.3$ g · s cm^{-3}).

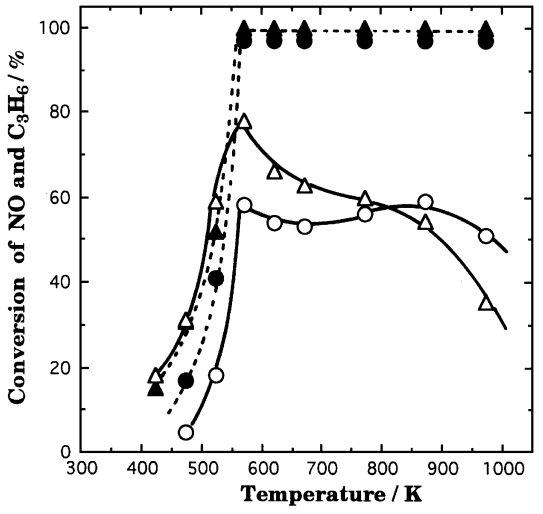

FIG. 10. Activity of Cu–SAPO-34 for NO and NO_2 reduction with C_3H_6 ($P_{NO\ or\ NO_2} = 1000$ ppm, $P_{C_3H_6} = 1000$ ppm, $P_{O_2} = 5\%$). NO–C_3H_6: (○) NO conversion, (●) C_3H_6 conversion. NO_2–C_3H_6: (△) NO_2 conversion, (▲) C_3H_6 conversion.

Cu–SAPO-34 exhibits high activity for NO reduction with C_3H_6 even in an atmosphere containing 15 vol% H_2O. Although the conversion to N_2 was slightly decreased within the initial 10 h, decreases in conversion to N_2 as well as C_3H_6 conversion were negligibly small over the examined 70 h. It is also noted that the constancy in the local and long-range order of Al, P, and Si in SAPO-34 could be recognized by the NMR and XRD measurements, respectively, after NO reduction for 70 h in a wet atmosphere. Therefore, the high activity of Cu–SAPO-34 for NO selective reduction with C_3H_6 was stably sustained for a long period, even in an atmosphere containing a fairly large amount of water vapor.

Activity of Cu–SAPO-34 for NO_2 Selective Reduction with C_3H_6

Figure 10 shows the temperature dependences of the activity of Cu–SAPO-34 for selective reduction of NO or NO_2 with C_3H_6. Yogo and Kikuchi reported that Ga ion-exchanged ZSM-5 exhibits a higher activity for NO_2 reduction than for NO reduction (24). Similarly to this result with Ga-ZSM-5, Cu–SAPO-34 exhibits a higher activity for NO_2 reduction than for NO reduction over the whole temperature range examined. In particular, conversion of NO_2 to N_2 attained a value as high as 80% at 573 K, as shown in Fig. 10.

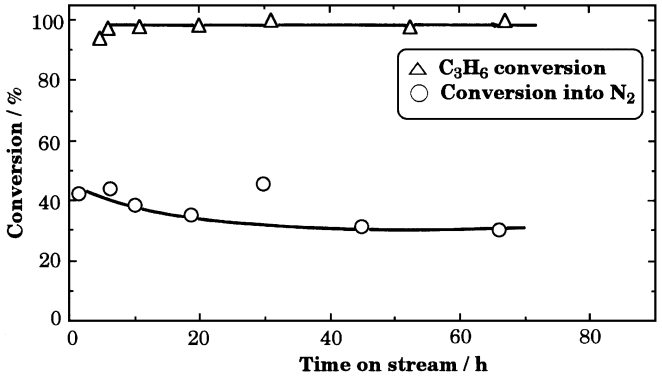

FIG. 9. Conversion into N_2 on Cu–SAPO-34 as a function of time on stream ($P_{NO} = 1000$ ppm, $P_{C_3H_6} = 1000$ ppm, $P_{O_2} = 5\%$, $P_{H_2O} = 15\%$).

Oxidation State of Cu in SAPO-34 after Heat Treatment in C_3H_6, NO, and O_2

It has been reported that the valence of Cu in ZSM-5 changes between monovalent and divalent during direct decomposition of NO and that the adsorbed NO is reduced to N_2 by the redox behavior of the Cu ion (25). Reduction of Cu(II) to Cu(I) during the selective reduction of NO with hydrocarbon has also been pointed out in the case of Cu–ZSM-5 (26). Therefore, it is expected that the redox behavior of the Cu ion has an important role also for the selective reduction of NO. ESR gives useful information on the oxidation state of copper (27). Figure 11 shows the ESR spectra of Cu in SAPO-34 after heating at 623 K, 1 h in C_3H_6, NO, and O_2. ESR signals assignable to Cu(II) were observed on Cu–SAPO-34 after evacuation at 523 K (Fig. 11a). Furthermore, two kinds of hyperfine structure possessing different *g* values were observed, suggesting that Cu(II) is dispersed at the atomic level in two different environments. Two kinds of Cu(II) in SAPO-34 were also reported by Zamadics *et al.* (28) and assigned to Cu(II) existing near the plane of the six-membered ring and Cu(II) in the hexagonal prism. These ESR signals assigned to Cu(II) almost disappeared after heating in C_3H_6 at 623 K for 1 h (Fig. 11b). Although it is reported that the ESR spectra of

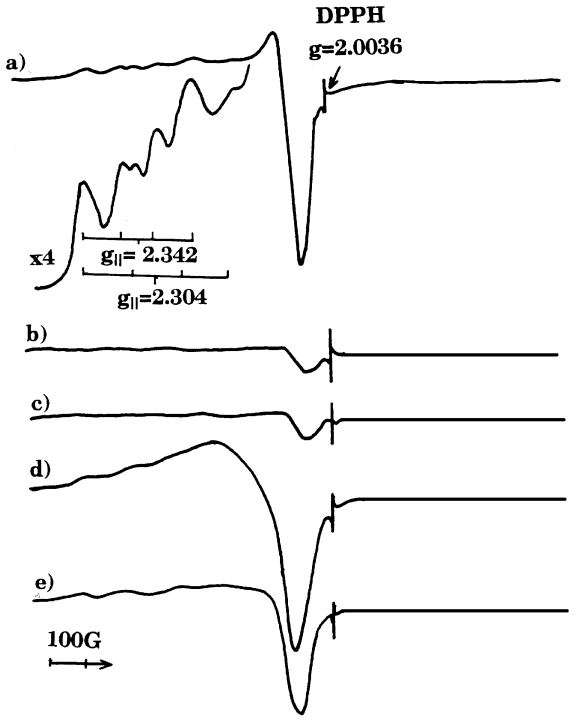

FIG. 11. ESR spectra of Cu–SAPO-34 after various treatments. (a) 773 K, 5 h evacuation → 673 K, 4 h, in O_2 (100 Torr) → 623 K, 3 h evacuation. (b) 623 K, 1 h in C_3H_6 (30 Torr) → 298 K evacuation. (c) 623 K, 5 h in NO (200 Torr) → 298 K evacuation. (d) 623 K, 5 h in O_2 (200 Torr) → 298 K evacuation. (e) Quenched in He during NO reduction ($P_{NO} = 1000$ ppm, $P_{C_3H_6} = 100$ ppm, $P_{O_2} = 5\%$, 623 K, 5 h).

Cu(II) ions reappear by exposure to NO in the case of Cu–Y zeolite reduced with CO (29), no changes were observed after subsequent exposure of Cu–SAPO-34 to NO at 623 K (Fig. 11c). This suggests that the reduced state of Cu formed by C_3H_6 treatment is stable in SAPO-34 in contrast to that in Y zeolite; however, the ESR signals assigned to Cu(II) as well as the hyperfine structure were partially restored by calcination at 623 K for 5 h in O_2 (Fig. 11d) and almost fully restored after treatment with O_2 for a further long period. In addition, it is noted that no significant amount of carbon was deposited during C_3H_6 treatment as judged by the XPS measurement for the same treatment. Since the ESR signal of Cu(II) was restored by the oxidizing treatment, the initial disappearance by C_3H_6 treatment (Fig. 11b) is not due to the aggregation of Cu ions but to the reduction of Cu(II). Similar changes in ESR spectra on heat treatment of C_3H_6 have been reported for Cu ion-exchanged KY (30) and ZSM-5 zeolite (31), where it was also concluded that C_3H_6 readily reduces ion-exchanged Cu(II). Thus, copper ions in SAPO-34 are also easily reduced on exposure to C_3H_6. Figure 11e shows the ESR spectra of Cu–SAPO-34 quenched in He during NO selective reduction with C_3H_6 at 623 K. Since Kucherov *et al.* reported that no measurable change of cupric cations occurs in a flow of pure He up to 773 K in the case of ZSM-5 (31), it is expected that no

TABLE 1

XPS Binding Energy of Cu $2p_{3/2}$ Electrons in Cu–SAPO-34 after Heating in O_2 and C_3H_6

	Binding energy (eV)		
	Cu $2p_{3/2}$	Shake-up line	Remarks
Cu–SAPO-34	934.0	942.9	Heated in O_2 at 623 K, 1 h
Cu–SAPO-34	932.5		Heated in C_3H_6 at 623 K, 1 h
Cu–SAPO-34	932.6		After reaction
Cu	932.2		
Cu_2O	932.8		
CuO	934.3	943.0	

reduction occurred during the quenching in He. Although the ESR signals assigned to Cu(II) were still observed, the double integral of the signal in Fig. 11e was far smaller than that of as-prepared Cu–SAPO-34 in Fig. 11a. This suggests that part of the Cu(II) in SAPO-34 remains in a reduced state under the selective reduction of NO with C_3H_6.

The valence changes of Cu ions were further studied by XPS (Table 1), and typical Cu $2p_{3/2}$ spectra after the various treatments are shown in Fig. 12. The oxidation state of Cu

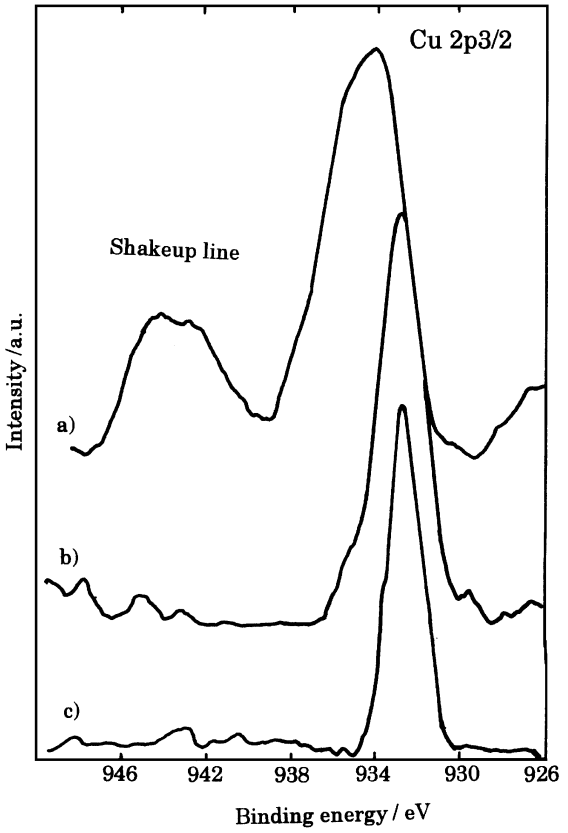

FIG. 12. XPS spectra of Cu $2p_{3/2}$ line of Cu–SAPO-34. (a) 723 K, 1 h in O_2 and then evacuation. (b) 723 K, 1 h in C_3H_6 and then evacuation. (c) Quenched in He during NO reduction ($P_{NO} = 1000$ ppm, $P_{C_3H_6} = 100$ ppm, $P_{O_2} = 5\%$, 623 K, 5 h).

in SAPO-34 seems to be Cu(II) after heating in O_2 at 723 K followed by evacuation to 10^{-7} Pa at room temperature, since the binding energy of Cu $2p_{3/2}$ (Table 1) and the Auger Cu LMM energy (335.3 eV) of Cu in SAPO-34 were almost consistent with those of CuO, and the shake-up satellite peaks were also observed in the binding energy range 940 to 950 eV as shown in Fig. 12a. Therefore, XPS measurements confirmed the results of ESR measurements and it is clear that the oxidation state of Cu in as-prepared SAPO-34 is divalent. C_3H_6 treatment at 723 K decreased the binding energy of the Cu $2p_{3/2}$ peak and slightly increased the Cu LMM energy; moreover, the XPS satellite peaks disappeared (Fig. 12b). The XPS spectrum was now similar to that of Cu_2O, but not that of metallic Cu or CuO, so Cu(II) in SAPO-34 is reduced to Cu(I) by C_3H_6 treatment. Although the oxidation number of Cu after the heating, in C_3H_6 could not be determined by ESR, the reduced state shown by ESR seems to be Cu(I) from the above XPS measurement. On the other hand, the XPS spectrum of Cu–SAPO-34 quenched during NO reduction at 623 K, 5 h closely resembled that of Cu–SAPO-34 treated with C_3H_6, although a weak shoulder was observed as shown in Fig. 12c. Considering the results of ESR, Cu(II) species also exist in SAPO-34 with reduced species of Cu on the quenched sample. It is most likely that the valence state of copper in SAPO-34 is a mixed state of monovalent and divalent under the selective reduction of NO. Facility in the monovalent-to-divalent redox of Cu ion also plays a key role in the reduction of NO in the case of direct NO decomposition on Cu–ZSM-5 (25) and NO selective reduction (32).

Chemisorption and Transformation of NO and C_3H_6 on Cu–SAPO-34

The adsorbed states of NO and C_3H_6 on Cu–SAPO-34 were investigated by infrared spectroscopy. Figure 13 shows the IR spectra of Cu–SAPO-34 after heating in NO, C_3H_6, and O_2 at 723 K. After adsorption of NO at 673 K, a strong absorption band at 1890 cm^{-1} and some weak absorption bands around 2200 and 1600 cm^{-1} were observed (Fig. 13a). The 1890 cm^{-1} band can be assigned to adsorbed NO, formed by donation of an electron from the antibonding orbital of NO, so adsorption of NO on Cu(II)–SAPO-34 is assumed to be reductive (33). The bands at 2240 and 2125 cm^{-1} are assigned to adsorbed N_2O and NO_2^+ species, respectively, in accordance with IR studies of adsorbed NO on Cu–ZSM-5 (33, 34) and CuO/SiO_2 (33, 35). Although bands around 1600 cm^{-1} were not observed in the IR spectra of adsorbed NO on Cu ion-exchanged ZSM-5 (34), absorption bands at 1600 and 1510 cm^{-1} can be assigned to the nitrate ion (NO_3^-) from the assignment of adsorbed NO on CuO/SiO_2 (35). The mass spectra of the gas phase taken at this stage consisted of a strong peak with mass number at 30, which was assigned to NO, and two weak peaks at 28 and 44, which corresponded to N_2 and N_2O, respectively. Therefore, the disproportionation of NO (for example, $3NO + Cu^+ = N_2 + Cu^{2+} + NO_{3\,ad}^-$ or $4NO + 2Cu^+ = N_2O + 2Cu^{2+} + 2NO_{3\,ad}^-$) seems to have occurred on Cu–SAPO-34 at 723 K to form adsorbed NO_3^- and gaseous N_2O and N_2. All absorption bands except those assigned to nitrate species disappear after evacuation of the gas phase at room temperature (Fig. 13b). Therefore, the adsorption of NO is extremely weak on Cu–SAPO-34.

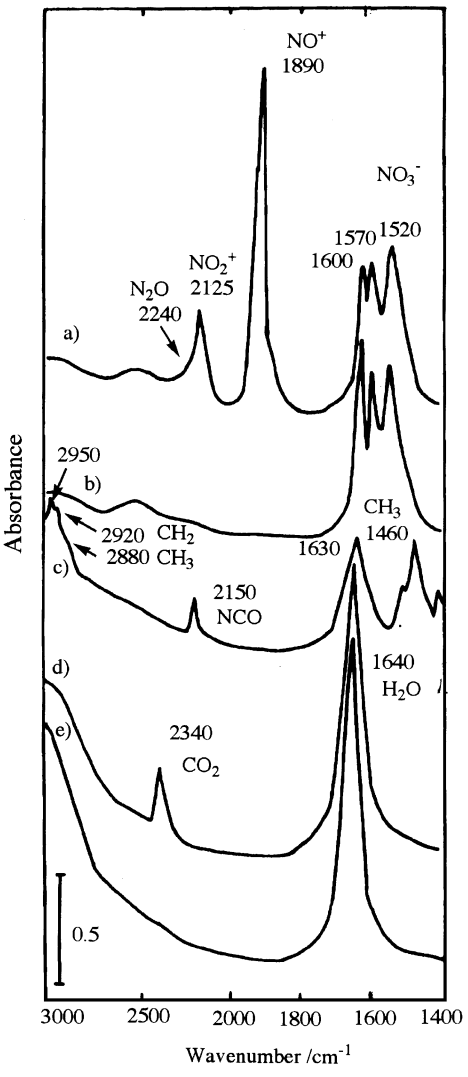

FIG. 13. IR spectra of Cu–SAPO-34 after exposure to NO, C_3H_6, and O_2. (a) Heating at 623 K, 3 h in NO (100 Torr). (b) Evacuation at 298 K. (c) Heating at 623 K, 6 h in C_3H_6 (30 Torr). (d) Calcination at 623 K, 1 h in O_2 (100 Torr). (e) Evacuation at 298 K.

Figure 13c shows the IR spectra after introduction of C_3H_6 at 623 K. The bands around 1600 cm^{-1} assigned to adsorbed nitrate species have completely disappeared, and new bands have appeared around 3000, 2250, 1640, 1450, and 1380 cm^{-1}. Absorption bands around 3000 cm^{-1} and those at 1450 and 1380 cm^{-1} can be assigned to the stretching and bending vibrations of CH_3 or CH_2 species

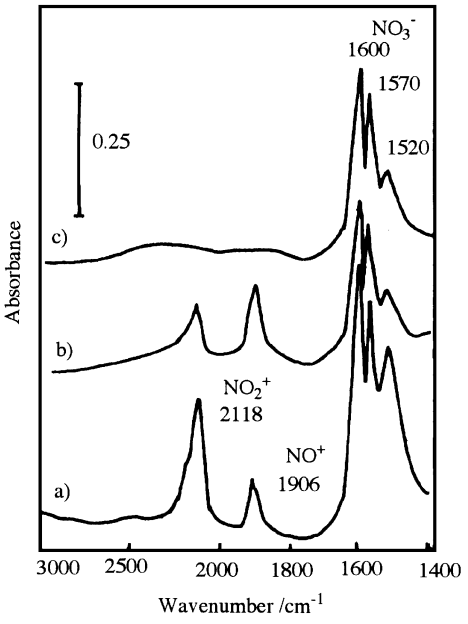

FIG. 14. IR spectra of Cu–SAPO-34 after exposure to NO_2. (a) Exposure to NO_2 (2.6 Torr) at 298 K. (b) Heating at 623 K, 3 h in NO_2 (2.6 Torr). (c) Evacuation at 295 K.

(36). CH_3 and CH_2 bands at these wavenumber values also appeared on H–SAPO-34 with almost the same absorbance after exposure to C_3H_6 at 623 K. Hence C_3H_6 adsorption on SAPO-34 may also be occurring on Brønsted acid sites in the present case. The band at 2250 cm^{-1} seems best assigned to NCO species, considering the results of similar experiments (34, 37, 38). Since the absorption bands left after NO treatment disappeared by the following C_3H_6 treatment, clearly the adsorbed nitrate species on Cu–SAPO-34 have readily reacted with C_3H_6. At present, it is not clear whether the adsorbed C_3H_6 reacted with adsorbed nitrate species as the carbonium ions of $C_3H_7^+$ or further dissociative species.

After evacuation of the gas phase, Cu–SAPO-34 was heated in oxygen at 723 K (Fig. 13d). The bands assigned to CH_2 or CH_3 species have disappeared and a band at 2340 cm^{-1}, which suggests the formation of gaseous CO_2, has appeared. Furthermore, it is expected that the formation of H_2O has also proceeded considering the strong absorption band at 1640 cm^{-1}. The formation of CO_2 was also confirmed by mass analysis of the gas phase in the IR cell.

Figure 14 shows the IR spectra of Cu–SAPO-34 after adsorption of NO_2 at room temperature. Absorption bands at 2118, 1906, 1600, 1570, and 1520 cm^{-1} appeared immediately after introduction of NO_2, even at room temperature. From the assignment in Fig. 13, the absorption bands at 2118 and 1906 cm^{-1} and three bands around 1600 cm^{-1} were assigned to NO_2^+, NO^+, and NO_3^- species, respectively. The formation of NO^+ and NO_3^- suggests that NO_2 was disproportionately adsorbed on Cu–SAPO-34 ($2NO_2 + Cu^+ = NO_{ad}^+ + Cu^{2+} + NO_{3\,ad}^-$). The bands of NO_3^- were observed only after heating to 723 K in the case of NO adsorption, whereas they were formed at temperatures as low as 298 K in the case of NO_2 adsorption. The activity of SAPO-34 ion-exchanged with Cu to NO selective reduction is higher than that of NO_2 as shown in Fig. 10. After evacuation of the gas phase, only three absorption bands around 1600 cm^{-1} remain (Fig. 14b). The following exposure to C_3H_6 and O_2 at 723 K gave the same IR spectra as shown in Figs. 13c and d. Therefore, except for the facility in NO_3^- formation, no significant differences were observed between NO_2 adsorption and NO adsorption. On the other hand, the formation of NO_3^- adsorbed species was promoted by reducing Cu–SAPO-34 by treatment with H_2 at 623 K. Therefore, it becomes clear that the reduced state of Cu ions in SAPO-34 exhibits a higher activity than Cu(II) ions for the NO disproportionation reaction and adsorbed NO_3^- was easily formed on the reduced Cu.

Since NO reduction by C_3H_6 did not proceed on Cu–SAPO-34 in the absence of O_2, oxygen seems to be involved in the formation of NO_3^- or the decomposition of organic nitro compounds as the intermediates. Although organic nitro compounds could not be detected in this study, the formation of adsorbed NCO species strongly supports formation of organic nitro compounds in the selective reduction of NO. The formation of CH_3NO_2 was also predicted on Cu–ZSM-5 in selective reduction of NO with C_3H_6 (38). Therefore, it is expected that the activity for the formation of NO_3^- is of primary importance for the selective reduction of NO with C_3H_6.

In fact, the reduction rate of NO with C_3H_6 increased with increasing partial pressure of NO and O_2 on the order of 0.77 and 0.36, respectively, but almost independent of increasing C_3H_6 partial pressure (the order is 0.05) at 473 K, at which selective reduction of NO with C_3H_6 dominated. Figure 15 shows the specific rate of C_3H_6 and NO

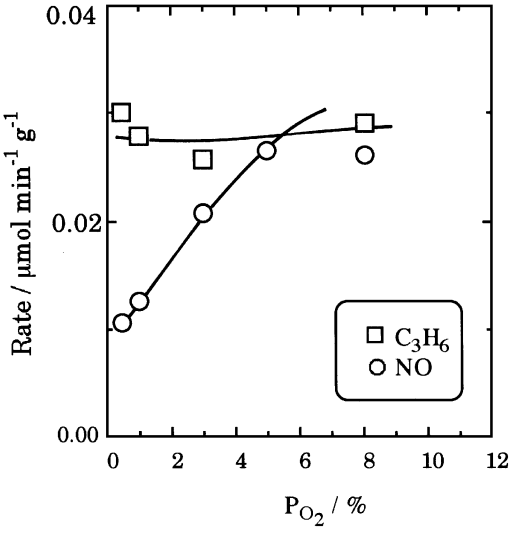

FIG. 15. Effect of O_2 partial pressure on the NO reduction rate and C_3H_6 consumption rate at 473 K ($P_{NO} = 1000$ ppm, $P_{C_3H_6} = 1000$ ppm).

consumption rate at 473 K as a function of oxygen partial pressure. Increasing oxygen partial pressure increased the NO consumption rate, but the effect on the C_3H_6 consumption rate was rather small. These results suggest that the reaction between NO and O_2, namely, the formation of NO_3^- on Cu(II), is the rate-determining step and that adsorption of C_3H_6 on Cu–SAPO-34 occurred readily. This is also in good agreement with the higher activity of Cu–SAPO-34 for the reduction of NO_2 than NO. The reaction mechanisms of NO selective reduction over Cu–SAPO-34 are under investigation.

4. CONCLUSION

In conventional studies on the catalysis of reactions by SAPO-*n*, only the properties of acidity or ion exchange have so far been applied; however, the crystal structure of SAPO-*n* or $AlPO_4$-*n* is thermally so stable that it is maintained up to 1273 K. Therefore, one of the promising applications of SAPO-*n* or $AlPO_4$-*n* is as a thermostable catalyst. Thermostable catalysts with high activity for NO reduction are critical to the development of catalysts for removal of NO_x by hydrocarbons. This study has revealed that Cu ion-exchanged SAPO-34 is promising as a thermostable catalyst for NO_x removal by hydrocarbons in an oxidizing atmosphere. High activity is maintained for a long period with Cu–SAPO-34, even in an atmosphere containing a fairly large amount of H_2O.

ACKNOWLEDGMENTS

Part of this study was financially supported by a Grant-in Aid for Science Research from the Ministry of Education, Science, and Culture of the Japanese Government, Nissan Science Foundation, and Kumagaya Research Foundation.

REFERENCES

1. Wilson, S. T., Lok, B. M., Messina, C. A., Cannon, T. R., and Flanigen, E. M., *Am. Chem. Soc. Symp. Ser.* **218**, 79 (1983).
2. Watanabe, Y., Koiwai, A., Takeguchi, H., Hyodo, S., and Noda, S., *J. Catal.* **143**, 430 (1993).
3. Misono, M., and Kondo, K., *Chem. Lett.*, 1001 (1991).
4. Cho, B. Y., *J. Catal.* **142**, 418 (1993).
5. Li, Y., Battavio, P. J., and Armor, J. N., *J. Catal.* **142**, 561 (1993).
6. Li, Y., and Armor, J. N., *J. Catal.* **145**, 1 (1994).
7. Hosose, H., Yahiro, H., Mizuno, N., and Iwamoto, M., *Chem. Lett.*, 1859 (1991).
8. Breck, D. W., "Zeolite Molecular Sieves." Krieger, FL.
9. Kharas, K. C. C., Robota, H. J., and Liu, D. J., *Appl. Catal. B* **2**, 225 (1993).
10. Armor, J. N., and Farris, T. S., *Appl. Catal. B* **4**, L11 (1994).
11. Ishihara, T., Kagawa, M., Hadama, F., and Takita, Y., *Stud. Surf. Sci. Catal. B* **84B**, 1493 (1994).
12. Wasowicz, T., Kim, S. J., Hong, S. B., and Kevan, L., *J. Phys. Chem.* **100**, 15954 (1996).
13. Panayotov, D., Dimitrov, L., Khristova, M., Petrov, L., and Mehandjiev, D., *Appl. Catal. B* **6**, 61 (1995).
14. Ciric, J., U.S. Patent 3972983 (1973).
15. Lok, B. M., Messina, C. A., Patton, R. L., Gajek, R. T., Cannon, T. R., and Flanigen, E. M., U.S. Patent 4440871 (1984).
16. Sato, S., Yu-u, Y., Yahiro, H., Mizuno, N., and Iwamoto, M., *Appl. Catal.* **70**, L1 (1991).
17. Briend, M., Peltre, M. J., Lamy, P. P., and Barthomeuf, D. B., *J. Catal.* **138**, 90 (1992).
18. Van Ballmoos, R., and Higgis, J. B., *Zeolites* **10**, 386 (1990).
19. Sanz, J., and Serratosa, J. M., *J. Am. Chem. Soc.* **106**, 4790 (1984).
20. Kustanovich, I., and Goldfarb, D., *J. Phys. Chem.* **95**, 8818 (1991).
21. Klinowski, J., *Chem. Rev.* **91**, 1459 (1993).
22. Briend, M., Peltre, M. J., Massiani, P., Man, P. P., Vomscheid, R., Derewinski, M., and Barthomeuf, D., "Zeolite and Related Microporous Materials: State of the Art 1994," p. 613. Elsevier, Amsterdam, 1994; Vomscheid, R., Briend, M., Peltre, M. J., Massiani, P., Man, P. P., and Barthomeuf, D., *J. Chem. Soc. Chem. Commun.*, 544 (1993).
23. Maistriau, L., Dumon, J., Nagy, J. B., Gabelica, Z., and Derouane, E. G., *Zeolites* **10**, 243 (1990).
24. Yogo, K., and Kikuchi, E., *Stud. Surf. Sci. Catal.* **84**, 1547 (1994).
25. Giamello, E., Murphy, D., Magnacca, G., Morterra, C., Shioya, Y., Nomura, T., and Anpo, M., *J. Catal.* **136**, 510 (1992).
26. Kharas, K. C. C., Liu, D. J., and Robota, H. J., *Catal. Today* **26**, 129 (1995).
27. Baird, J. C., and Bersohn, M., "An Introduction to Electron Paramagnetic Responce." Benjamin, Elmsford, NY, 1996.
28. Zamadics, M., Chen, X., and Kevan, L., *J. Phys. Chem.* **96**, 2652 (1992).
29. Chao, C., and Lunsford, J. H., *J. Phys. Chem.* **76**, 1546 (1972).
30. Sung, J., and Kevan, L., *J. Phys. Chem.* **94**, 7612 (1990).
31. Kucherov, A. V., Gerlock, J. L., Jen, H., and Shelef, M., *J. Phys. Chem.* **98**, 4892 (1994).
32. Inui, T., Kojo, S., Masaki, S., Yoshida, T., and Iwamoto, S., *Stud. Surf. Sci. Catal.* **69**, 355 (1991).
33. Arai, H., and Tominaga, H., *J. Catal.* **43**, 131 (1976).
34. Yahiro, Y., Yu-u, Y., Takeda, Y., Mizuno, N., and Iwamoto, M., *Shokubai* **35**, 130 (1993).
35. London, J. W., and Bell, A. T., *J. Catal.* **31**, 96 (1973).
36. Silvi, B., Labarbe, P., and Perchard, J. P., *Spectrochim. Acta Part A* **29**, 263 (1973).
37. Hecker, W. C., and Bell, A. T., *J. Catal.* **85**, 389 (1984).
38. Yokoyama, C., Yasuda, M., and Misono, M., *J. Catal.* **150**, 9 (1994).